

DESIGN AND OPTIMIZATION OF PLANAR MULTILAYER ANTIREFLECTION METAMATERIAL COATINGS AT KU BAND UNDER CIRCULARLY POLARIZED OBLIQUE PLANE WAVE INCIDENCE

H. Oraizi and A. Abdolali

Department of Electrical Engineering
Iran University of Science and Technology
Narmak, Tehran 1684613114, Iran

Abstract—In this paper, planar multilayered antireflection coatings composed of isotropic and dispersive common materials and metamaterials (DPS, DNG, ENG, and MNG) are designed and optimized at Ku band under circularly polarized oblique plane wave incidence by a full-wave method and combination of the method of least squares (MLS), genetic algorithm (GA) and conjugate gradients (CG). The body on which the coating is applied may be selected as PEC, plexiglas, or any other material. As a result a new class of radar absorbing materials (RAM) are obtained, which may be effectively used for antireflection coatings. Furthermore, guidelines are presented for the selection of correct signs for the real and imaginary parts of propagation constant k and intrinsic impedance η .

1. INTRODUCTION

Reduction of radar cross-section (RCS) has been realized by several methods, such as radar absorbing materials (RAMs) [1, 2]. However, RAMs have various other applications, such as anechoic chambers, low side-lobe level antennas, and protection and shielding of high frequency circuits from electromagnetic interference. Initially, RAMs were employed as a single quarter wave layer, which were narrow band. Later, multilayer quarter wave RAMs were devised to broaden the frequency response. In 1994 ideal RAMs were designed by perfect matched layers (PMLs) [3–6], but impedance matching could not be realized at all angles of incidence and general polarization.

In this paper we investigate the applicability of combinations of common materials (DPS) and metamaterials (DNG, ENG, and MNG) as RAMs. Veselago first hypothesized DNG materials, where the

real parts of permittivity (ϵ) and permeability (μ) were negative, which were also referred to as left handed (LH) materials [7]. The structures and methods of fabrication of DNG, ENG and MNG metamaterials and wave propagation in such media are described in the literature [8–15]. In this paper we are concerned with the macroscopic properties of metamaterials as embodied in the Drude, Lorentz and resonance models. Consequently, we consider the dispersion properties of metamaterials, whereby the values of ϵ and μ are highly dependent on frequency [16]. However, we use a combination of DPS, DNG, ENG, and MNG materials for multilayered coatings. The MLS and the combination of minimization algorithms of GA and CG are used for the design and optimization of RCSs by RAMs. The design parameters are the thicknesses of layers and the parameters in the dispersion relations of ϵ and μ of the selected materials. The design examples are divided into (1) normal incidence in a wide frequency band, (2) oblique incidence at a wide range of angles and at a single frequency, and (3) a wide range of incident angles and a wide frequency band simultaneously.

2. NUMERICAL PROCEDURE

There are various methods for analysis of multilayered structures [17–24], we follow the procedure developed in [25] for the analysis of multilayered planar structures (with n layers) as shown in Fig. 1.

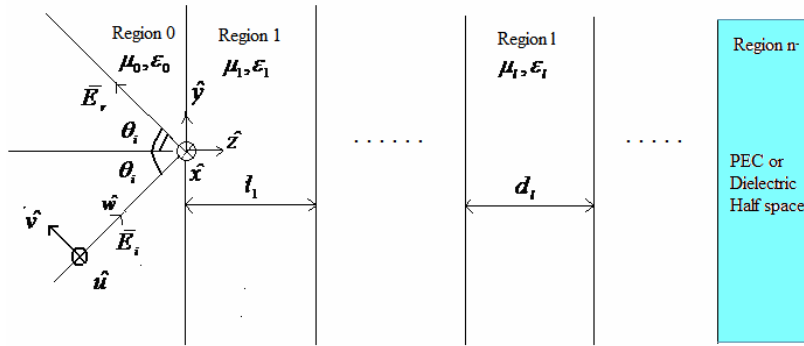


Figure 1. A multilayered planar medium.

Consider an elliptically polarized plane wave (which may be decomposed into TE and TM waves) obliquely incident under an arbitrary angle of incidence on the structure. The TE and TM waves are defined by E_{lx} and H_{lx} in the l th layer, respectively. For the TE

wave, we have (with the time dependence as $e^{j\omega t}$)

$$\text{TE} \begin{cases} H_{\ell y} = \frac{1}{j\omega\mu_\ell} \frac{\partial}{\partial z} E_{\ell x} \\ H_{\ell z} = \frac{-1}{j\omega\mu_\ell} \frac{\partial}{\partial y} E_{\ell x} \\ \left(\frac{\partial^2}{\partial y^2} + \frac{\partial^2}{\partial z^2} + \omega^2\mu_\ell\varepsilon_\ell \right) E_{\ell x} = 0 \end{cases} \quad (1)$$

$$E_x = E_0 e^{-jK_z z - jK_y y} \quad (2)$$

where the characteristic equation is obtained from the Helmholtz equation. The total field in the l th layer is the superposition of two forward and backward ($\pm z$ directions) traveling waves:

$$E_{\ell x} = (E_\ell^- e^{jK_{\ell z} z} + E_\ell^+ e^{-jK_{\ell z} z}) e^{-jK_y y} \quad (3)$$

$$H_{\ell y} = \frac{K_{\ell z}}{\omega\mu_\ell} (E_\ell^- e^{jK_{\ell z} z} - E_\ell^+ e^{-jK_{\ell z} z}) e^{-jK_y y} \quad (4)$$

$$H_{\ell z} = \frac{K_y}{\omega\mu_\ell} (E_\ell^- e^{jK_{\ell z} z} + E_\ell^+ e^{-jK_{\ell z} z}) e^{-jK_y y} \quad (5)$$

$$K_{\ell z}^2 + K_y^2 = \omega^2\mu_\ell\varepsilon_\ell \quad (6)$$

where E_l^+ and E_l^- are the respective field amplitudes in the l th layer. In the half space in front of the multilayer structure $l = 0$ and

$$E_0^+ = E_0 \quad (7)$$

$$E_0^- = RE_0 \quad (8)$$

where R is the reflection coefficient. Evoking the boundary conditions (namely the continuity of tangential electric and magnetic fields over the boundaries between adjacent layers) leads to a set of linear equations for the unknown field amplitudes for n layers. There are $n+1$ boundaries which lead to $2(n+1)$ equations for $2(n+1)$ unknown amplitudes. Consequently, a recursive relation is obtained for $\frac{E_l^-}{E_l^+}$ in term of $\frac{E_{l+1}^-}{E_{l+1}^+}$ which leads to the computation of a closed form equation

for the reflection coefficient.

$$\begin{aligned}
R = & \frac{e^{j2k_{oz}d_1}}{R_{0l}} + \frac{\left[1 - \left(\frac{1}{R_{01}^2}\right)\right] e^{j2(k_{1z}+k_{0z})d_1}}{\left(\frac{1}{R_{01}}\right) e^{j2k_{1z}d_1}} \\
& + \frac{e^{j2k_{1z}d_2}}{R_{12}} + \frac{\left[1 - \left(\frac{1}{R_{12}^2}\right)\right] e^{j2(k_{2z}+k_{1z})d_2}}{\left(\frac{1}{R_{12}}\right) e^{j2k_{2z}d_2}} + \dots \\
& + \frac{e^{j2k_{(n-1)z}d_n}}{R_{(n-1)n}} + \frac{\left[1 - \left(\frac{1}{R_{(n-1)n}^2}\right)\right] e^{j2(k_{nz}+k_{(n-1)z})d_n}}{\left(\frac{1}{R_{(n-1)n}}\right) e^{j2k_{nz}d_n}} \\
& + R_{nt} e^{j2k_{nz}d_{(n+1)}}
\end{aligned} \tag{9}$$

where

$$P_{\ell(\ell+1)} = \frac{\mu_{\ell} K_{(\ell+1)z}}{\mu_{\ell+1} K_{\ell z}} \tag{10}$$

$$R_{\ell(\ell+1)} = \frac{1 - P_{\ell(\ell+1)}}{1 + P_{\ell(\ell+1)}} \tag{11}$$

Similar relations may be obtained for the TM polarization by duality:

$$\bar{E}_{\ell} \rightarrow \bar{H}_{\ell}, \quad \bar{H}_{\ell} \rightarrow -\bar{E}_{\ell}, \quad \mu_{\ell} \rightarrow \varepsilon_{\ell}$$

For the circular polarization of the incident plane wave, we have [26]:

$$\bar{E}_i = (E_{ui}\hat{u} \pm jE_{vi}\hat{v}) = E_0 e^{-jK_z z - jK_y y} (\hat{u} \pm j\hat{v}) \tag{12}$$

where \pm denotes left-handed and right-handed waves, respectively (for $e^{j\omega t}$ time dependence). Consequently, the reflected wave will have an elliptical polarization as

$$\bar{E}_r = (E_{ur}\hat{u} \mp jE_{vr}\hat{v}) \tag{13}$$

The RCS may be written as reflectance.

$$\text{Reflectance} = \frac{|E_r|^2}{|E_i|^2} \tag{14}$$

where

$$\begin{aligned} |E_r|^2 &= |E_{ur}|^2 + |E_{vr}|^2 \\ |E_i|^2 &= |E_{ui}|^2 + |E_{vi}|^2 = 2E_0^2 \end{aligned} \quad (15)$$

If we have normal incident, then:

$$E_z = 0, u \rightarrow x, v \rightarrow y$$

3. OPTIMIZATION BY THE COMBINATION OF MLS, GA AND CG

We have proposed the combination of genetic algorithm and conjugate gradient algorithm to minimize the error function in the method of least squares. The error functions in scattering problems have many extrema [27]. Locating the global minimum by merely GA is very time consuming [28–30] and by merely CG is likely to get trapped in a local minimum. Consequently, we use GA to start the algorithm and proceed towards the vicinity of a local minimum, where the algorithm is switched to CG, to rapidly converge to the local minimum. Then GA is activated to migrate to the vicinity of other minima, and the same procedure is repeated. Therefore, both the advantages of GA for searching the global minimum and that of CG for rapid convergence towards a local minimum are benefited and their disadvantages of slow convergence of GA and local search nature of CG are avoided. It is noted that the convergence of CG is highly dependent on the initial values of variables. In the proposed minimization procedure, the values obtained by GA act as the initial values for CG, which highly speeds up its convergence.

The MLS error function is defined as [31]:

$$\text{Error Function} = \sum_{j=1}^{n_\theta} \sum_{i=1}^{n_f} W_{ij} [\text{Reflectance}(f_i, \theta_j) - C_{ij}]^2 \quad (16)$$

where C_{ij} is the desired reflectance at frequency f_i , θ_j is angle of incidence, n_f is the number of frequencies in the band, n_θ is the number of discrete incident angles and W_{ij} is the weighting factor relating to C_{ij} .

4. MATERIALS AND METAMATERIALS FOR RAMS

Various materials and metamaterials may be used for coating of objects as RAMs. Such materials may be lossless or lossy and in general their

dispersion characteristics should be taken into account. According to the sign of the real parts of permittivity ($\varepsilon = \varepsilon' - j\varepsilon''$) and permeability ($\mu = \mu' - j\mu''$), the materials are categorized into four classes (namely DPS, DNG, ENG, and MNG). The dispersion relations of several types of right handed (RH) and left handed (LH) materials, which may have applications for RAMs are given in Table 1 [32].

Table 1. List of materials used in the design of RAMs. (Frequencies in dispersion relations are in terms of GHz).

Class of materials	Permittivity model	Permeability model	Parameters Ranges
Lossy dielectric	$\varepsilon = \frac{\varepsilon_r}{f^\alpha} - j\frac{\varepsilon_i}{f^\beta}$	$\mu = \mu_r$	$1 \leq \varepsilon_r, \varepsilon_i, \mu_r \leq 25$ $0 \leq \alpha, \beta \leq 1$
Relaxation-type magnetic	$\varepsilon = \varepsilon_r$	$\mu = \frac{\mu_m(f_{mp}^2 - jf_m f)}{f^2 + f_m^2}$	$1 \leq \varepsilon_r \leq 25$ $1 \leq \mu_m \leq 25$ $1 \leq f_m \leq 33$
Rods only	$\varepsilon = 1 - \frac{f_{ep}^2}{f^2 - jf\gamma_e}$	$\mu = 1$	$1 \leq f_{ep} \leq 33$ $0.001 \leq \gamma_e \leq 7$
Rings only	$\varepsilon = 1$	$\mu = 1 - \frac{f_{mp}^2 - f_{mo}^2}{f^2 - f_{mo}^2 - jf\gamma_m}$	$1 \leq f_{mo} \leq 33$ $f_{mp} \sim f_{mo} + [0.1, 5]$ $0.001 \leq \gamma_m \leq 7$

5. CORRECT SIGN OF WAVE NUMBER k AND WAVE IMPEDANCE η

When the real parts of ε and μ are positive, the values of k and η may be directly computed by their relations without much ado, namely $k = \omega\sqrt{\mu\varepsilon}$ and $\eta = \sqrt{\mu/\varepsilon}$.

However, for metamaterials DNG, ENG and MNG, their correct signs should be selected due to the fact that the square root of a complex number is two valued. The sign depends on the time dependence (here as $e^{+j\omega t}$) and space dependence (here as $e^{-j\vec{k}\cdot\vec{r}}$). In this case, for losses (rather than amplification) to occur, the imaginary parts of ε and μ should be negative. Accordingly, the correct signs for the real and imaginary parts of k and η for the lossy and lossless materials are given in Tables 2 and 3, respectively. If the time and space dependencies are reversed, some signs may change [33]. The computer programs are written in such a way as to closely check the various conditions and select the correct signs for ε and μ . For example,

Table 2. Correct signs of k and η for lossy materials ($\varepsilon', \varepsilon'', \mu', \mu'', \eta', \eta'', k', k''$, are positive parameters).

	ε	μ	k	η
DPS	$+\varepsilon' - j\varepsilon''$	$+\mu' - j\mu''$	$+k' - jk''$	$+\eta' \pm j\eta''$
DNG	$-\varepsilon' - j\varepsilon''$	$-\mu' - j\mu''$	$-k' - jk''$	$+\eta' \pm j\eta''$
ENG	$-\varepsilon' - j\varepsilon''$	$+\mu' - j\mu''$	$\pm k' - jk''$	$+\eta' + j\eta''$
MNG	$+\varepsilon' - j\varepsilon''$	$-\mu' - j\mu''$	$\pm k' - jk''$	$+\eta' - j\eta''$

Table 3. Correct signs for η and k for lossless materials.

	ε	μ	k	η
DPS	$+\varepsilon'$	$+\mu'$	$+k'$	$+\eta'$
DNG	$-\varepsilon'$	$-\mu'$	$-k'$	$+\eta'$
ENG	$-\varepsilon'$	$+\mu'$	$-jk''$	$+j\eta''$
MNG	$+\varepsilon'$	$-\mu'$	$-jk''$	$-j\eta''$

for the lossless metamaterials, the value computed for k by the formula $k = \omega\sqrt{\mu\varepsilon}$ should be multiplied by a negative sign, and for MNG, the sign of the value computed for η by the formula $\eta = \sqrt{\mu/\varepsilon}$ should be changed.

6. NUMERICAL EXAMPLES

First, for the verification of the proposed MLS-GA-CG procedure for RAMs design, we consider an example treated in the literature to compare the results [34]. The reflectance for the reflected power and transmittance for the transmitted power relative to the incident power are defined as follows.

$$\text{reflectance} = \frac{|\text{reflected wave amplitude}|^2}{|\text{incident wave amplitude}|^2} \tag{17}$$

$$\text{transmittance} = 1 - \frac{|\text{reflected wave amplitude}|^2}{|\text{incident wave amplitude}|^2} = 1 - \text{reflectance} \tag{18}$$

Example 1. Computation of transmittance of a 21-planar-layers under TE polarization and incident angles $\theta_i = 0, 20^\circ, 40^\circ$

We consider a structure composed of 21 planar layers placed in free space. The thickness of each layer is a quarter wave length

of the center frequency in free space. The permittivities of layers are periodically equal to ε_H and ε_L . Therefore, the structure is designated as $(HL)^{10}H$. Here $\varepsilon_H = 5.0625$, $\varepsilon_L = 2.1025$ are equivalent to $n_H = 2.25$, $n_L = 1.45$. The thickness of layers is $d = 3.75$ mm. Transmittance is computed in the band 100–300 GHz for the incident angles $\theta_i = 0, 20^\circ, 40^\circ$ and drawn in Fig. 2. The results of computations by the proposed method completely coincide with those of reference [34]. The same problem was analyzed for TM polarization, and perfect match was obtained with reference [34].

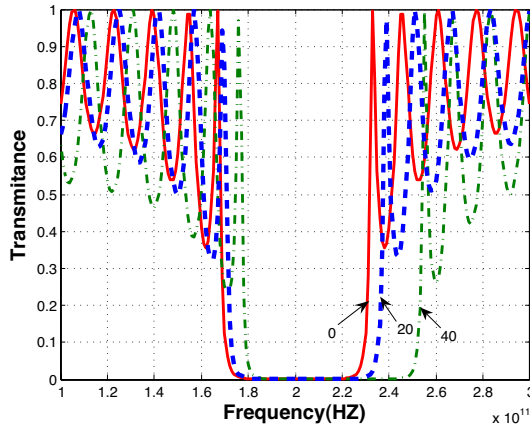


Figure 2. Transmittance versus frequency for a $(HL)^{10}H$ dielectric planar multilayer structure placed in free space with TE polarization and various incident angles for example 1.

Example 2. Reduction of reflectance by a single layer coating under normal incidence at Ku band

Consider a PEC plane covered by a single layer coating of dispersive material. The conditions for minimization of reflectance from the structure are studied. First, the increase of layer thickness often results in the reduction of reflectance. Second, it is observed that the application of MTMs are best for the reduction of reflectance. This is an interesting observation which may be used to devise RAM structures for the reduction of reflectance and RCS. The reflectance versus frequency is drawn in Fig. 3 for five types of single layer coatings and circular polarization. The thicknesses of layers and parameters of dispersion relations are given in Table 4. Furthermore, the minimization of reflectance was performed at a single frequency for the angles of incidence in the range $0 < \theta < 90^\circ$. Again, it was observed that MTMs were the best for the reduction of reflectance. However,

in such problems, the increase of thickness does not necessarily lead to the reduction of reflectance.

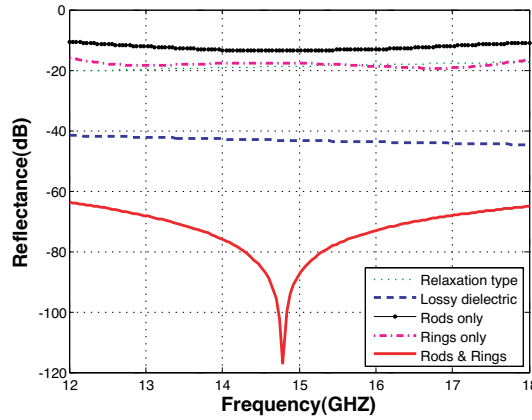


Figure 3. Reflectance of a PEC plane with a thick layer of coating for example 2.

Table 4. Layer thicknesses and parameters of dispersion relations for example 2.

Class of materials	Thickness (mm)	Parameters of dispersion relations
Relaxation-type	30	$\epsilon_r = 3.5276, \mu_m = 3.9686,$ $f_m = 29.8 \text{ GHz}$
Lossy dielectric	30	$\epsilon_r = 25, \epsilon_i = 7.1942,$ $\alpha = 5.0163 \times 10^{-7},$ $\beta = 0.8990, \mu_r = 24.91$
Rods only	30	$f_{ep} = 10.9384 \text{ GHz},$ $\gamma_e = 5 \text{ GHz}$
Rings only	30	$f_{mo} = 14.3461 \text{ GHz},$ $f_{mp} = 15.6628 \text{ GHz}, \gamma_m = 5 \text{ GHz}$
Rods & Rings	30	$f_{ep} = 29.997 \text{ GHz}, \gamma_e = 4.9126 \text{ GHz}$ $f_{mo} = 1 \text{ GHz}, f_{mp} = 29.945 \text{ GHz},$ $\gamma_m = 4.8901 \text{ GHz}$

Example 3. Reduction of reflectance by a single layer coating on a PEC plate over a wide frequency band and a wide range of incident angles

Several materials were used for the coating. Optimum designs were obtained for metamaterials. The 3-D diagram for the best case namely rods & rings metamaterial is shown in Fig. 4 and the related data for parameter values are given Table 5. The reduction of reflectance in this example is less than the former example 2, because here the reflectance is minimized over a wide frequency band and a wide range of incident angles.

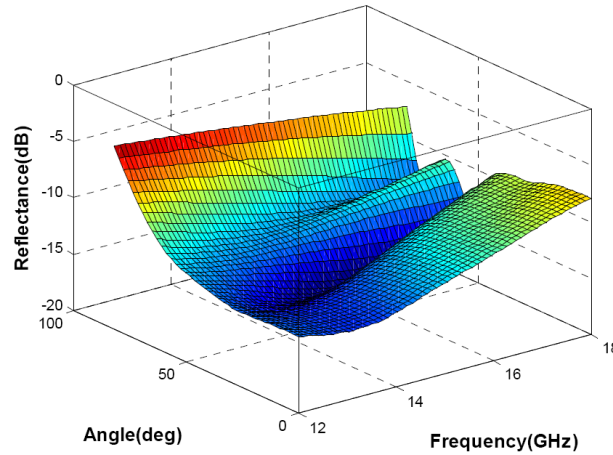


Figure 4. Reflectance of a PEC plane covered by a single MTM layer coating for example 3.

Table 5. Layer thickness and parameters of dispersion relations for example 3.

Class of materials	Thickness (mm)	Parameters of dispersion relations
Rods & Rings	30	$f_{ep} = 5.7366$ GHz, $\gamma_e = 0.0011$ GHz $f_{mo} = 9.0325$ GHz, $f_{mp} = 3$ GHz, $\gamma_m = 4.979$ GHz

Example 4. Reduction of reflectance by a two-layer-coating for normal incidence at Ku band

This example is the same as the former example 3, except that here there are two layers of coating. Reduction of reflectance by MLS was carried out for 30 cases of combinations of RH and LH materials. Only the best 4 cases of design and minimization of reflectance are

shown in Fig. 5. The related data are given in Table 6. Again it is shown that metamaterials are the best for RAMs. Here rods & rings metamaterial has the best performance for the reduction of reflectance.

Table 6. Thicknesses of layers and parameters of dispersion relations for example 4.

Class of materials	Thickness (mm)	Parameters of dispersion relations
Layer 1: Rings only	27.034	$f_{mo} = 14.225$ GHz, $f_{mp} = 15.041$ GHz, $\gamma_m = 5$ GHz
Layer 2: Rods only	30	$f_{ep} = 13.576$ GHz, $\gamma_e = 4.971$ GHz
Layer 1: Relaxation-type	1.458	$\epsilon_r = 4.0563$, $\mu_m = 5.7108$, $f_m = 19.872$ GHz
Layer 2: Rods & Rings	30	$f_{ep} = 12.814$ GHz, $\gamma_e = 5$ GHz $f_{mo} = 18.486$ GHz, $f_{mp} = 3$ GHz, $\gamma_m = 0.22938$ GHz
Layer 1: Lossy dielectric	2.4539	$\epsilon_r = 15.5903$, $\epsilon_i = 1.2562$, $\alpha = 0.1576$, $\beta = 0.9832$, $\mu_r = 10.1839$
Layer 2: Rods & Rings	29.993	$f_{ep} = 25.582$ GHz, $\gamma_e = 4.785$ GHz $f_{mo} = 1.001$ GHz, $f_{mp} = 25.580$ GHz, $\gamma_m = 4.970$ GHz
Layer 1: Rods & Rings	30	$f_{ep} = 18.075$ GHz, $\gamma_e = 4.980$ GHz $f_{mo} = 1$ GHz, $f_{mp} = 18.057$ GHz, $\gamma_m = 4.954$ GHz
Layer 2: Rods & Rings	29.997	$f_{ep} = 14.289$ GHz, $\gamma_e = 4.999$ GHz, $f_{mo} = 17.870$ GHz, $f_{mp} = 14.469$ GHz, $\gamma_m = 0.029$ GHz

Example 5. Reduction of reflectance by a two-layer-coating at a wide frequency band under a wide range of incident angles for circular polarization

This example is similar to example 3, but it is composed of two layers of coating. The advantage of two-layer-coating is that by the combination of different types of metamaterials, it is possible to drastically reduce reflectance by thinner coatings. Two cases of bilayer coatings namely rods & rings-relaxation type and rods & rings-rods & rings are designed and optimized for minimum reflectance. Their wide

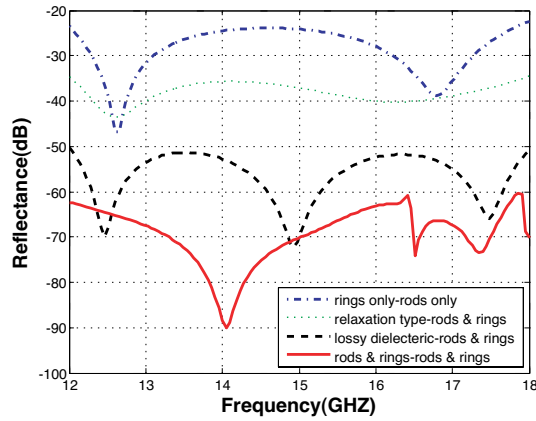


Figure 5. Reflectance from a PEC plane covered by two layers of coating made of various combinations of RH and LH materials for example 4.

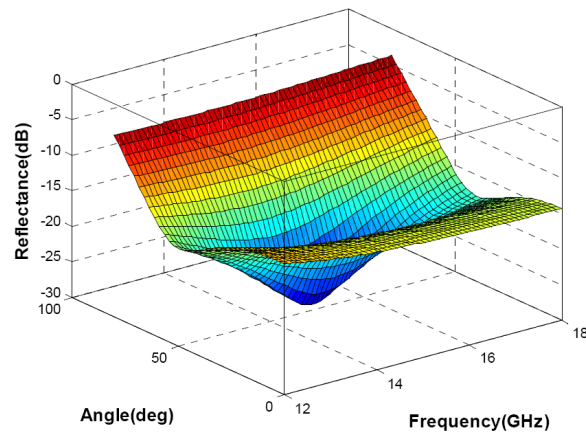


Figure 6. Reflectance from a PEC plate with two layers of coating made of rods & rings — Relaxation type material for example 5.

angle frequency responses are shown in Figs. 6 and 7. The related data are given in Table 7. Again the advantages of metamaterials for applications as RAMs are noteworthy.

Example 6. Reduction of reflectance from a plexiglas plate with an MTM layer at Ku band for a wide range of incident angles for a circularly polarized plane wave

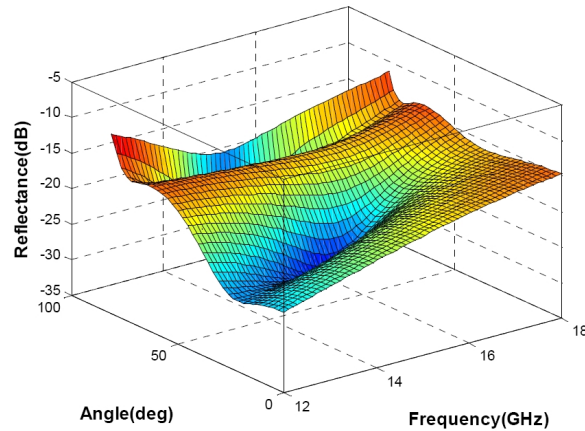


Figure 7. Reflectance from a PEC plate with two layers of coating made of rods & rings MTM for example 5.

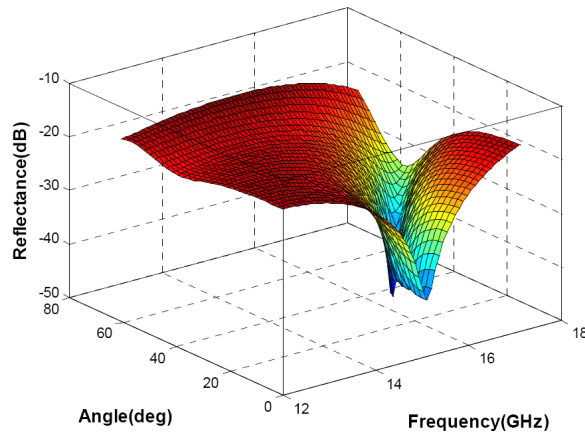


Figure 8. Reflectance from a plexiglas plate covered by an MTM coating versus frequency and angle of incidence for circularly polarized plane wave.

The plexiglas plate has constants ($\epsilon_r = 2.7$, $\mu_r = 1$) and thickness = 20 mm. The minimization of reflectance has been carried out at Ku band over the range of incident angles $0 < \theta < 90^\circ$. The 3-D reflectance response versus frequency and incident angles is shown in Fig. 8. The relevant data are given in Table 8. It is again observed that metamaterials are more effective than common materials as RAMs for reduction of RCS.

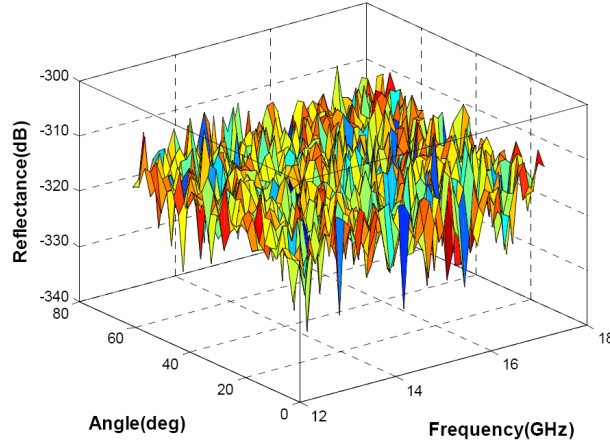


Figure 9. Reflectance from a plexiglas plate covered by a nondispersive MTM coating versus frequency and angle of incidence for circularly polarization of incident plane wave (example 7).

Table 7. Thicknesses of layers and parameters of dispersion relations for RH and LH materials for example 5.

Class of materials	Thickness (mm)	Parameters of dispersion relations
Layer 1: Rods & Rings	0.259	$f_{ep} = 32.9$ GHz, $\gamma_e = 5.89$ GHz $f_{mo} = 12.684$ GHz, $f_{mp} = 21.3017$ GHz, $\gamma_m = 6.2$ GHz
Layer 2: Relaxation-type	0.6042	$\epsilon_r = 10.075$, $\mu_m = 12.398$, $f_m = 15.565$ GHz
Layer 1: Rods & Rings	13.639	$f_{ep} = 1.001$ GHz, $\gamma_e = 6.899$ GHz $f_{mo} = 26.304$ GHz, $f_{mp} = 27.416$ GHz, $\gamma_m = 6.989$ GHz
Layer 2: Rods & Rings	1.6072	$f_{ep} = 32.854$ GHz, $\gamma_e = 6.999$ GHz $f_{mo} = 1.005$ GHz, $f_{mp} = 34.196$ GHz, $\gamma_m = 7$ GHz

Example 7. Invisible plexiglas at all frequencies and any incident angles

Consider the same plexiglas slab as in example 6, where $\epsilon_r = 2.7$, $\mu_r = 1$ and thickness = 10 mm. If a metamaterial slab with symmetrical parameters $\epsilon_r = -2.7$, $\mu_r = -1$ and the same thickness is placed on it,

Table 8. Thickness of layer and dispersion parameters of MTM coating on a Plexiglas plate for example 6.

Class of materials	Thickness (mm)	Parameters of dispersion relations
Rods & Rings	5.87	$f_{ep} = 1 \text{ GHz}$, $\gamma_e = 0.0012 \text{ GHz}$ $f_{mo} = 10.033 \text{ GHz}$, $f_{mp} = 9.1863 \text{ GHz}$, $\gamma_m = 6.48 \text{ GHz}$

tunneling occurs and as shown in Fig. 9, reflection is nearly zero. This phenomenon may be described as the following theorem.

Theorem: If two slabs of the same thickness made of lossless materials with symmetrical electric and magnetic parameter ($t_1 = t_2$, $\varepsilon_{r1} = -\varepsilon_{r2}$, $\mu_{r1} = -\mu_{r2}$) are placed side by side, then the reflection from such a structure would be zero.

7. CONCLUSION

The formulation in [25] for the analysis of planar multilayered MTM structures is extended for the lossy dispersive RH/LH materials for the reduction of reflectance and RCS under TE, TM and circularly polarized plane wave incidence for a wide frequency band and wide angles of incidence. For the minimization of reflectance, the combination of MLS, GA and CG was used for various examples. If it is desired to reduce the reflectance at a single frequency at a particular angle of incidence, it may be accomplished even by more than 100 dB. However, it was observed that the application of MTMs lead to a significant reduction of reflectance for a general polarization of the incident plane wave and in a wide frequency band and wide angles of incidence. Consequently, the conclusions in this study is (as in other references) a further evidence of the potential applications of MTMs for the drastic reduction of RCS of various objects. It is seen that the application of two layers of coatings of different MTMs with less thickness may lead to more reduction of reflectance as compared to a thicker single layer of coating.

Furthermore, some guidelines for the selection of correct signs for propagation constant k and intrinsic impedance η of lossless and lossy metamaterials are presented.

REFERENCES

1. Vinoy, K. J. and R. M. Jha, *Radar Absorbing Materials: From Theory to Design and Characterization*, Kluwer Academic Publishers, Norwell, Massachusetts, 1996.
2. Chen, X. J. and X. W. Shi, "Comments on a formula in radar cross section," *Journal of Electromagnetic Waves and Applications*, Vol. 21, No. 15, 2389–2394, 2007.
3. Berenger, J.-P., "A perfectly matched layer for the absorption of electromagnetic waves," *Journal of Computational Physics*, 114–185, 1994.
4. Chew, W. C. and W. H. Weedon, "A 3D perfectly matched medium from modified Maxwell's equations with stretched coordinates," *Microwave Opt. Technol. Lett.*, Vol. 7, No. 13, 599–604, 1994.
5. Chew, W. C., J. M. Jin, and E. Michielssen, "Complex coordinate stretching as a generalized absorbing boundary condition," *Microwave Opt. Technol. Lett.*, Vol. 15, No. 6, 363–369, 1997.
6. Jancewicz, B., "Plane electromagnetic wave in PEMC," *Journal of Electromagnetic Waves and Applications*, Vol. 20, No. 5, 647–659, 2007.
7. Veselago, V. G., "The electrodynamics of substances with simultaneously negative values of ε and μ ," *Soviet Physics Uspekhi*, Vol. 10, No. 4, 509–514, 1968.
8. Pendry, J. B., A. J. Holden, D. J. Robbins, and W. J. Stewart, "Low frequency plasmons in thin-wire structures," *J. Phys. Condens. Matter*, Vol. 10, 4785–4809, 1998.
9. Pendry, J. B., A. J. Holden, D. J. Robbins, and W. J. Stewart, "Magnetism from conductors and enhanced nonlinear phenomena," *IEEE Trans. on Micr. Theory. Tech.*, Vol. 47, No. 11, 2075–1084, 1999.
10. Smith, D. R., W. J. Padilla, D. C. Vier, S. C. Nemat-Nasser, and S. Schultz, "Composite medium with simultaneously negative permeability and permittivity," *Phys. Rev. Lett.*, Vol. 84, No. 18, 184–4187, 2000.
11. Caloz, C. and T. Itoh, *Electromagnetic Metamaterials: Transmission Line Theory and Microwave Applications*, Wiley Interscience, New Jersey, 2006.
12. Chen, H., B. I. Wu, and J. A. Kong, "Review of electromagnetic theory in left-handed materials," *Journal of Electromagnetic Waves and Applications*, Vol. 20, No. 15, 2137–2151, 2006.

13. Engheta, N. and R. W. Ziolkowski, "A positive future for double-negative metamaterials," *IEEE Trans. Microwave Theory Tech.*, Vol. 53, No. 4, 1535–1556, 2005.
14. Lu, J., B. I. Wu, J. A. Kong, and M. Chen, "Guided modes with a linearly varying transverse field inside a left-handed dielectric slab," *Journal of Electromagnetic Waves and Applications*, Vol. 20, No. 5, 689–697, 2006.
15. Villa-Villa, F., J. Gaspar-Armenta, and A. Mendoza-Suárez, "Surface modes in one dimensional photonic crystals that include left handed materials," *Journal of Electromagnetic Waves and Applications*, Vol. 21, No. 4, 485–499, 2007.
16. Manzanares-Martinez, J. and J. Gaspar-Armenta, "Direct integration of the constitutive relations for modeling dispersive metamaterials using the finite difference time-domain technique," *Journal of Electromagnetic Waves and Applications*, Vol. 21, No. 15, 2297–2310, 2007.
17. Ghaffari-Miab, M., A. Farmahini-Farahani, R. Faraji-Dana, and C. Lucas, "An efficient hybrid swarm intelligence-gradient optimization method for complex time Green's functions of multilayer media," *Progress In Electromagnetics Research*, PIER 77, 181–192, 2007.
18. Yla-Oijala, P., M. Taskinen, and J. Sarvas, "Multilayered media Green's functions for MPIE with general electric and magnetic sources by the Hertz potential approach," *Progress In Electromagnetics Research*, PIER 33, 141–165, 2001.
19. Naqvi, Q. A. and A. A. Rizvi, "Fractional solutions for the Helmholtz's equation in a multilayered geometry," *Progress In Electromagnetics Research*, PIER 21, 319–335, 1999.
20. Yin, W. Y., G. H. Nan, and I. Wolff, "The combined effects of chiral operation in multilayered bianisotropic substrates," *Progress In Electromagnetics Research*, PIER 20, 153–178, 1998.
21. Berginc, G., C. Bourrely, C. Ordenovic, and B. Torr'esani, "A numerical study of absorption by multilayered biperiodic structures," *Progress In Electromagnetics Research*, PIER 19, 199–222, 1998.
22. Shaarawi, A. M., I. M. Besieris, A. M. Attiya, and E. El-Diwany, "Reflection and transmission of an electromagnetic X-wave incident on a planar air-dielectric interface: Spectral analysis," *Progress In Electromagnetics Research*, PIER 30, 213–249, 2001.
23. Asole, F., L. Deias, and G. Mazzarella, "A flexible full-wave analysis of multilayered AMC using an aperture oriented

- approach,” *Journal of Electromagnetic Waves and Applications*, Vol. 21, No. 14, 2059–2072, 2007.
24. Guney, K., C. Yildiz, S. Kaya, and M. Turkmen, “Synthesis formulas for multilayer homogeneous coupling structure with ground shielding,” *Journal of Electromagnetic Waves and Applications*, Vol. 21, No. 14, 2073–2084, 2007.
 25. Kong, J. A., “Electromagnetic wave interaction with stratified negative isotropic media,” *Progress In Electromagnetics Research*, PIER 35, 1–52, 2002.
 26. Tah-Hsiung, C., “Polarization effects on microwave imaging of dielectric cylinder,” *IEEE Transactions on Microwave Theory and Techniques*, Vol. 36, No. 9, 1366–1369, 1988.
 27. Oraizi, H. and A. Abdolali, “Ultra wide band RCS optimization of multilayered cylindrical structures for arbitrarily polarized incident plane waves,” *Progress In Electromagnetics Research*, PIER 78, 129–157, 2008.
 28. Rahmat-Samii, Y. and E. Michielssen, *Electromagnetic Optimization by Genetic Algorithms*, Wiley, New York, 1999.
 29. Tian, Y.-B. and J. Qian, “Ultra-conveniently finding multiple solutions of complex transcendental equations based on genetic algorithm,” *Journal of Electromagnetic Waves and Applications*, Vol. 20, No. 4, 475–488, 2006.
 30. Zhai, Y. W., X. W. Shi, and Y. J. Zhao, “Optimized design of ideal and actual transformer based on improved micro-genetic algorithm,” *Journal of Electromagnetic Waves and Applications*, Vol. 21, No. 13, 1761–1771, 2007.
 31. Oraizi, H., “Application of the method of least squares to electromagnetic engineering problems,” *IEEE Antenna and Propagation Magazine*, Vol. 48, No. 1, 50–75, 2006.
 32. Michielssen, E., J.-M. Sajer, S. Ranjithan, and R. Mittra, “Design of lightweight, broad-band microwave absorbers using genetic algorithms,” *IEEE Trans. Microwave Theory Tech.*, Vol. 41, No. 67, 1024–1031, 1993.
 33. Oraizi, H. and A. Abdolali, “Combination of MLS, GA & CG for the reduction of RCS of multilayered cylindrical structures composed of dispersive metamaterials,” *Progress In Electromagnetics Research B*, Vol. 3, 227–253, 2008.
 34. Cory, H. and C. Zach, “Wave propagation in metamaterial multilayered structures,” *Microwave and Optical Technology Letters*, Vol. 40, No. 6, 460–465, 2004.